PERGAMON

Deep-Sea Research II 49 (2002) 149–174

DEEP-SEA RESEARCH
PART II

www.elsevier.com/locate/dsr2

A deterministic model for N_2 fixation at stn. ALOHA in the subtropical North Pacific Ocean

Katja Fennel[a,*], Yvette H. Spitz[a], Ricardo M. Letelier[a], Mark R. Abbott[a], David M. Karl[b]

[a] *College of Oceanic and Atmospheric Sciences, Oregon State University, 104 Ocean Administration Building, Corvallis, OR 97331, USA*

[b] *School of Ocean and Earth Science and Technology, University of Hawaii, Honolulu, HI 96822, USA*

Abstract

Marine N_2 fixation by diazotrophic microorganisms is a key process in biogeochemical cycling and yields an important input of new nitrogen into the tropical and subtropical surface ocean. However, it is only poorly accounted for in current numerical models. We present a simple biological model that explicitly includes N_2 fixation by diazotrophic phytoplankton. The model employs a mechanistic parameterization of N_2 fixation based on physiological responses of *Trichodesmium* to physical conditions of the environment. The model is conceived to allow shifts in nitrogen versus phosphorus control of the plankton community by resolving the biogeochemical cycles of both elements. Typical N : P ratios were assigned to the different functional groups to capture variations in the N : P stoichiometries of inorganic and organic matter pools. The biological model was coupled to a 1D physical model of the upper ocean. A simulation was performed at stn. ALOHA (22°45′N, 158°W) in the subtropical North Pacific Ocean, where intense blooms of *Trichodesmium* occurred during the last decade. The model captures essential features of the biological system including the vertical structure and seasonal course of chlorophyll, the seasonal cycle and interannual differences in diazotrophic biomass, the mean vertical particle flux, and an oscillation in the relative importance of nitrogen versus phosphorus. We regard this model as a step towards a mechanistic tool to assess the magnitude of marine N_2 fixation and to explore hypotheses on its effect on carbon sequestration from the atmosphere. © 2001 Published by Elsevier Science Ltd.

1. Introduction

The importance of marine N_2 fixation by diazotrophic phytoplankton in the present ocean has been stressed in several recent studies (Carpenter and Romans, 1991; Capone et al., 1997;

*Corresponding author. Tel.: +1-541-737-3281; fax: +1-541-737-2064.
E-mail address: kfennel@coas.oregonstate.edu (K. Fennel).

0967-0645/01/$ - see front matter © 2001 Published by Elsevier Science Ltd.
PII: S0967-0645(01)00098-4

Falkowski, 1997; Karl et al., 1997; Capone and Carpenter, 1999; Karl et al., 2001a). N_2 fixation by *Trichodesmium*, which is a dominant diazotroph in tropical and subtropical waters, yields an important input into the global nitrogen cycle (Capone et al., 1997), as it supplies a significant fraction of new nitrogen in the subtropical Pacific (Karl et al., 1997), the tropical North Atlantic (Carpenter and Romans, 1991), and the Arabian Sea (Capone et al., 1998). Furthermore, the aperiodic appearance of large *Trichodesmium* blooms observed during the Hawaii ocean time-series (HOT) program has been recognized as an important source of biogeochemical variability in the subtropical Pacific. The massive occurrence of *Trichodesmium* changed the elemental composition of organic matter pools (Karl et al., 1992) and potentially switches the system from a nitrogen to a phosphorus limited state (Karl et al., 1997). The admitted importance of marine N_2 fixation has prompted speculation about its effect on the oceanic draw-down of atmospheric CO_2 by altering the export of carbon from surface waters (Hood et al., 2000).

N_2 fixation acts as a negative feedback mechanism in the global nitrogen cycle and might directly affect the partitioning of carbon between the atmosphere and the ocean (Falkowski, 1997). On long time scales of thousands of years, N_2 fixation, which is selected for by low N : P ratios and repressed by high N : P ratios, represents a mechanism to constrain ecological stoichiometry close to the Redfield ratio (Lenton and Watson, 2000). In the present ocean, phosphate is available in slight excess relative to nitrate (Tyrrell, 1999) and N_2 fixation represents a net source of fixed nitrogen in the global nitrogen cycle. N_2 fixation in turn is controlled by the available phosphorus, iron (a requirement for the enzyme nitrogenase), and oxygen (a potent inhibitor of nitrogenase). This input of new nitrogen drives the biological system from the current nitrogen limitation towards limitation by phosphorus, and potentially affects the magnitude of carbon sequestration from the atmosphere. Since on average only the biogenic material based on new nutrients can be exported from the upper ocean, the export of carbon by the biological pump depends directly on the supply of new nutrients.

Modeling efforts directed towards a better understanding of marine biogeochemical cycles and their response to anthropogenic perturbations have increased considerably in recent years. However, the achievement of long-term goals, like the prediction of carbon sequestration from the atmosphere by the oceans, still requires substantial improvements of the currently available numerical models. One main task is the better representation of functional diversity and multi-elemental cycling to capture major shifts in biogeochemical mechanisms (Doney, 1999). N_2 fixation is a key process that is not yet represented well in present models.

Here we present a simple model that explicitly describes the functional behavior of diazotrophs. The model includes the elemental cycling of nitrogen and phosphorus to allow a differentiation between nitrogen and phosphorus control and simulates the effect of N_2 fixation on the N : P stoichiometry in the euphotic zone. The phytoplankton community is divided into two functional groups, diazotrophs represented by *Trichodesmium* and other phytoplankton, which are characterized by different stoichiometric ratios. This variable treatment of N : P stoichiometries leads to an uncoupling of the nitrogen and phosphorus cycles. The parameterization of N_2 fixation is based on observed physiological responses of *Trichodesmium* to environmental conditions. Effects of temperature, irradiance, and wind speed are taken into account. The ecological model is coupled to a one-dimensional physical model of the upper water column at stn. ALOHA (22°45′N, 158°W) in the subtropical North Pacific Ocean. This site represents an excellent test case for a modeling study not only because a comprehensive set of physical and

biological data are simultaneously collected during the HOT field program (Karl and Lukas, 1996), but also because dramatic changes in the microbial community structure, in particular massive blooms of *Trichodesmium*, occurred during the observational program. These blooms alter nutrient cycling mechanisms and stoichiometries of inorganic and organic matter pools (Karl et al., 1997). The present model is intended as a step towards a mechanistic simulation tool that allows a future assessment of the magnitude of marine N_2 fixation and an exploration of hypotheses on the effect of N_2 fixation on the sequestration of atmospheric CO_2.

2. Previous approaches used to model N_2 fixation

Parameterizations for the input of nitrogen into the oceanic system by N_2 fixation have been employed previously by Bissett et al. (1999), Tyrrell (1999), Hood et al. (2001) and Neumann (2000). The model of Bissett et al. (1999) implicitly accounts for N_2 fixation as a flux to the dissolved organic matter pool. The authors implemented a simple parameterization assuming a nitrogen source that is proportional to temperature and irradiance while diazotrophic biomass is not included explicitly. In contrast, Hood et al. (2001) explicitly model *Trichodesmium* biomass. Nitrogen uptake by *Trichodesmium* is simulated depending only on irradiance. Bioavailable fixed nitrogen and dinitrogen are utilized alternatively by *Trichodesmium* with increased dinitrogen uptake when reactive nitrogen is depleted. Since phosphate is essential for plankton growth and becomes increasingly important if N_2 fixation occurs, the omission of phosphate in the parameterizations of Bissett et al. (1999) and Hood et al. (2001) is viewed as a major deficiency. The elemental ratio of reactive nitrogen and phosphorus in the ocean is close to the Redfield ratio ($N : P = 16$ mol : mol) on global average, with regional variations associated with N_2 fixation and denitrification (Lenton and Watson, 2000). Marine phytoplankton are typically considered as limited by fixed nitrogen, since phosphate is generally available in slight excess to inorganic nitrogen relative to demand (Codispoti and Berger, 1989). N_2 fixation provides a mechanism that releases the phytoplankton community from nitrogen limitation and thus gives rise to phosphorus limitation of phytoplankton growth.

Tyrrell (1999) describes the cycling of nitrogen and phosphorus in a simplified model that presents the global ocean in two homogeneous boxes. The N_2 fixation rate in this model is determined by the supply ratio of dissolved inorganic nitrogen and phosphorus. This approach is based on the ecological consideration that diazotrophs are selected for during periods when reactive nitrogen is scarce relative to phosphate. Neumann (2000) takes a mechanistic approach to describe the cycling of nitrogen and phosphorus in a three-dimensional coupled model of the Baltic Sea. The N_2 fixation rate of the diazotrophs in this model (dominant species in the Baltic Sea are *Aphanizomenon* and *Nodularia*; Wasmund, 1997) is determined depending on phosphate supply, temperature and irradiance. The approaches of Tyrrell (1999) and Neumann (2000) are, in principle, capable of distinguishing between nitrogen and phosphorus control of phytoplankton growth. Both assume a fixed ecological stoichiometry of 16N : 1P implying a tight coupling of the nitrogen and phosphorus cycles. However, dramatic variations from the canonical Redfield ratio in dissolved, suspended and sinking organic matter pools have been observed during periods of enhanced N_2 fixation (Karl et al., 1992, 1997). Since these changes in elemental composition are likely to affect biogeochemical cycling of nitrogen, phosphorus and carbon, a more flexible

approach that allows changes in elemental stoichiometries is needed to account for shifts in biogeochemical processes.

3. Model description

A coupled one-dimensional physical/biological model is presented that describes the input of new nitrogen into the biological system by N_2 fixation. The model covers the euphotic and shallow subeuphotic zones of the upper water column (0–350 m). The evolution of any biological scalar C is given by

$$\frac{\partial C}{\partial t} = \frac{\partial}{\partial z}\left(K\frac{\partial C}{\partial z}\right) + \mathrm{sms}(C), \tag{1}$$

where the first term on the right-hand side accounts for vertical mixing, and the second term represents the biological "sources minus sinks" of the particular biological scalar (sms). The vertical diffusion coefficient, K, accounts for vertical mixing determined by the mixed-layer parameterization and a uniform background diffusion.

3.1. The physical model

The physical component of the coupled model simulates the vertical profiles of horizontal velocities, temperature, and salinity over time, the vertical mixing of the biological scalars, and the evolution of the mixed-layer depth in response to synoptical wind stresses and surface heat fluxes. It is a version of the mixed-layer model described by Price et al. (1986), which is modified by the inclusion of a uniform background diffusion to allow an upward eddy-diffusive flux of nutrients below the seasonal thermocline. The turbulent mixing due to surface forcing is given by a Richardson-number-dependent parameterization. In the model, mixing occurs to ensure the static stability of the water column and to satisfy stability criteria of the bulk Richardson-number and the gradient Richardson-number. A thorough description is given in Price et al. (1986). In addition to the surface mixing a uniform background diffusion is applied to parameterize the turbulent transport below the thermocline. The background mixing is the only mechanism in the model for the upward transport of nutrients below the mixed layer and, hence, is essential to maintain biological cycling in the euphotic zone. A vertical diffusion coefficient $K_{\mathrm{back}} = 5 \times 10^{-5}\ \mathrm{m^2\ s^{-1}}$ is applied which is at the upper end of the vertical diffusivities estimated for the HOT site (Christian et al., 1997).

The heat penetration of insolation is described by a double exponential depth dependence (Kraus, 1972) that includes a short- and a long-wave component of solar radiation. The attenuation parameters are chosen to represent the clear, mid-ocean water of the subtropical Pacific according to the Paulson and Simpson (1977) classification. The daily cycle of solar radiation is calculated from the classical astronomical formula (Brock, 1981) employing the correction of the solar constant by Duffie and Beckman (1980).

3.2. Concept of the biological model

The biological model contains seven state variables: the two nutrient pools, dissolved inorganic nitrogen (din) and dissolved inorganic phosphorus (dip), two phytoplankton groups, diazotroph nitrogen fixers (nif) and all other phytoplankton (phy), zooplankton (zoo), and the two detrital pools, detrital particulate nitrogen (det_N) and detrital particulate phosphorus (det_P) (Table 1). A schematic of the biological model is shown in Fig. 1. The elemental cycles of nitrogen and phosphorus are resolved. Due to the ability of the diazotrophs to utilize dinitrogen as an alternative nitrogen source the cycles of nitrogen and phosphorus are uncoupled. By fixation of dinitrogen, which is assumed here to be an unlimited source, new nitrogen is introduced into the nitrogen cycle. This input increases the pool of bioavailable nitrogen in the system in comparison to the corresponding pool of phosphorus.

We assume that the diazotrophs satisfy their nitrogen demand only by N_2 fixation without any uptake of dissolved inorganic or organic nitrogen, i.e. they are obligate diazotrophs. Although laboratory studies have shown that *Trichodesmium* (and probably other diazotrophs as well) can grow on fixed nitrogen compounds when present at sufficiently high concentrations (Ohki et al., 1991; Mulholland et al., 1999), nitrogen isotopic measurements of field collected *Trichodesmium* colonies generally confirm the condition of obligate diazotrophy (Wada and Hattori, 1991). Further support for our assumption of obligate diazotrophy is given by recent results from a field study at the Bermuda Atlantic Time-series Study (BATS) in the North Atlantic. In situ measurements of nitrogen incorporation by *Trichodesmium* have shown that the uptake of bound forms of nitrogen accounted for $<6\%$ compared to N_2 fixation throughout the year and even $<1\%$ during the summer months when *Trichodesmium* abundances were highest (Orcutt et al., 2001).

Our parameterization for diazotrophic growth captures the important physiological features of *Trichodesmium*, namely low growth and high respiration rates (Kana, 1992). *Trichodesmium* is common in waters between 20°C and 30°C and reaches its maximum growth rates in stable, stratified waters with high solar insolation (Carpenter and Romans, 1991; Capone et al., 1997). Doubling times are low between 20°C and 24°C, ranging from weeks to months (Mague et al., 1977; McCarthy and Carpenter, 1979; Carpenter et al., 1987). Turnover times increase rapidly for water temperatures above 25°C (Carpenter, 1983; Carpenter et al., 1987; Carpenter and Romans, 1991; Carpenter and Capone, 1992). An inverse relationship between wind speed and the rate of

Table 1
Model state variables

Symbol	Unit	Variable	Background value
din	mmol N m^{-3}	Dissolved inorganic nitrogen	
dip	mmol P m^{-3}	Dissolved inorganic phosphorus	
nif	mmol N m^{-3}	Diazotrophs	$nif_0 = 0.01$ mmol N m^{-3}
phy	mmol N m^{-3}	Other phytoplankton	$phy_0 = 0.01$ mmol N m^{-3}
zoo	mmol N m^{-3}	Zooplankton	$zoo_0 = 0.001$ mmol N m^{-3}
det_N	mmol N m^{-3}	Detrital particulate nitrogen	$det_{N0} = 0.001$ mmol N m^{-3}
det_P	mmol P m^{-3}	Detrital particulate phosphorus	$det_{P0} = 0.001$ mmol P m^{-3}

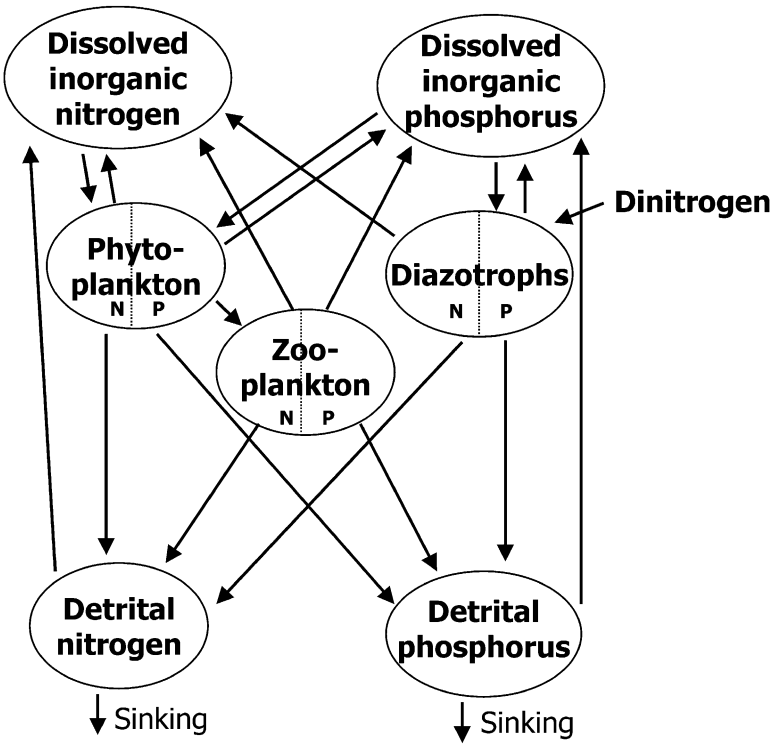


Fig. 1. Schematic of the biological model.

N_2 fixation has been reported by Bryceson and Fay (1981), Carpenter and Price (1977) and Wasmund (1997). The direct sensitivity of *Trichodesmium* to water column stability may arise from their morphological structure. *Trichodesmium* contains gas vacuoles that allow an active buoyancy regulation and a large fraction occurs in colonial form. Carpenter and Price (1977) have shown that N_2 fixation rates decrease with increasing disturbance which tends to break up colonies and Letelier and Karl (1998) report significantly reduced N_2 fixation rates for disrupted colonies. Based on the observational evidence, the effect of temperature and water-column stability is taken into account in the present model by a temperature and wind-stress-dependent growth amplification factor.

The elemental ratio of nitrogen versus phosphorus compounds in the phytoplankton community is commonly assumed to be close to the Redfield ratio. *Trichodesmium*, however, can achieve substantially higher stoichiometric N : P ratios during P-controlled growth. Letelier and Karl (1996) report a mean N : P ratio of 45 at stn. ALOHA, a ratio 3 times larger than the Redfield ratio. To account for this different stoichiometry the uptake and release processes of the diazotrophs are determined with a N : P ratio of 45 while a value close to Redfield is assumed for the other phytoplankton and zooplankton. The cellular stoichiometries are defined to be constant for each phytoplankton group.

Our model does not contain dissolved organic matter (DOM) pools and does not resolve the microbial recycling community. The microbial loop, which is sustained by rapid cropping of small

forms of phytoplankton by microzooplankton and by microbial assimilation of DOM pools, is an important component of the biological system as it provides a major part of the nitrogen and phosphorus taken up by primary producers (Azam, 1998). An explicit representation of these processes in the model would require a deterministic description of the nitrogen and phosphorus fluxes through the microbial community. Since the dynamics of the dissolved organic nitrogen and phosphorus pools are sufficiently complex and ill-constrained, a detailed mechanistic modeling of these interactions may be premature at this stage (Karl et al., 2001b). Instead, we account only indirectly for the microbial recycling by a remineralization flux that feeds directly into the inorganic nutrient pools.

3.3. Parameterization of the biological dynamics

The dynamics of the ecological state variables is determined by the following set of equations. The corresponding parameter values are given in Table 2. The biological sources and sinks of phytoplankton are defined by

$$\begin{aligned}\mathrm{sms(phy)} = {} & \mu_{\mathrm{phy}}(\mathrm{din}, \mathrm{dip}, E)\mathrm{phy} - \mu_{\mathrm{zoo}}(\mathrm{phy})\mathrm{zoo} - L_{\mathrm{phy,din}}(\mathrm{phy} - \mathrm{phy}_0) \\ & - L_{\mathrm{phy,det}}(\mathrm{phy} - \mathrm{phy}_0), \end{aligned} \tag{2}$$

Table 2
Model parameters[a]

Symbol	Value	Unit	Parameter
$L_{\mathrm{phy,din}}$	0.05	d^{-1}	Phytoplankton respiration rate
$L_{\mathrm{phy,det}}$	0.05	d^{-1}	Phytoplankton mortality rate
k_{N}	0.5	mmol N m^{-3}	Half-saturation concentration for din uptake
k_{P1}	0.0015	mmol P m^{-3}	Half-saturation concentration for dip uptake by phy
r_1	14	mol N : mol P	Stoichiometry of phy and zoo
$\mu_{\mathrm{phy}}^{\mathrm{max}}$	3.0	d^{-1}	Maximum growth rate of phy
α_1	0.07	$(\mathrm{W\ m}^{-2})^{-1}\ \mathrm{d}^{-1}$	Initial PI-slope of phy
$L_{\mathrm{nif,din}}$	0.17	$\mathrm{d}^{-1}\ (\mathrm{mmol\ N\ m}^{-3})^{-1}$	Diazotrophic respiration rate
$L_{\mathrm{nif,det}}$	0.05	d^{-1}	Diazotrophic mortality rate
$\mu_{\mathrm{nif}}^{\mathrm{max}}$	0.3	d^{-1}	Maximum growth rate of nif
k_{P2}	0.0004	mmol P m^{-3}	Half-saturation concentration for dip uptake by nif
α_2	0.01	$(\mathrm{W\ m}^{-2})^{-1}\ \mathrm{d}^{-1}$	Initial PI-slope of nif
T_{crit}	24.75	°C	Critical temperature
τ_{crit}	0.062	N m^{-2}	Critical windstress
r_2	45	mol N : mol P	Stoichiometry of nif
$\mu_{\mathrm{zoo}}^{\mathrm{max}}$	1.0	d^{-1}	Maximum grazing rate of zoo
k_{phy}	0.25	$(\mathrm{mmol\ N\ m}^{-3})^2$	Half-saturation concentration for ingestion by zoo
γ	0.75	Dimensionless	Zooplankton assimilation efficiency
$L_{\mathrm{zoo,din}}$	0.05	d^{-1}	Zooplankton excretion rate
$L_{\mathrm{zoo,det}}$	0.05	$\mathrm{d}^{-1}\ (\mathrm{mmol\ N\ m}^{-3})^{-1}$	Zooplankton mortality rate
rem	0.01	d^{-1}	Remineralization rate
w_{det}	2.5	m d^{-1}	Sinking velocity of detritus

[a] The parameters agree with values in common use (cf. Spitz et al., 2001; Oschlies and Garçon, 1999; Doney et al., 1996; Fasham et al., 1990).

where the phytoplankton growth rate, μ_{phy}, depends on the concentrations of din and dip according to Michaelis–Menten kinetics and the availability of the photosynthetically active radiation, $F_{\mathrm{phy}}(E)$. The growth rate is given by

$$\mu_{\mathrm{phy}}(\mathrm{din},\mathrm{dip},E)=F_{\mathrm{phy}}(E)\min\left(\frac{\mathrm{din}}{k_{\mathrm{N}}+\mathrm{din}},\frac{\mathrm{dip}}{k_{\mathrm{P1}}+\mathrm{dip}}\right), \tag{3}$$

where k_{N} and k_{P1} are the half-saturation constants for the uptake of din and dip, respectively. According to Liebig's law of the minimum the growth rate is limited by either inorganic nitrogen or phosphorus, whichever is in shorter supply relative to need. $F_{\mathrm{phy}}(E)$ is determined following Evans and Parslow (1985)

$$F_{\mathrm{phy}}(E)=\frac{\mu_{\mathrm{phy}}^{\max}\alpha_1 E}{\sqrt{(\mu_{\mathrm{phy}}^{\max})^2+(\alpha_1 E)^2}}, \tag{4}$$

where $\mu_{\mathrm{phy}}^{\max}$ is the maximum growth rate of phytoplankton, and α_1 the initial slope of the PI-curve. E represents the fraction of light that is effective in photosynthesis and is exponentially decreasing with water depth. Effects of wavelength dependency and self-shading of chlorophyll are neglected. Phytoplankton loss terms are grazing by zooplankton and linear losses to the dissolved nutrient pools and the detritus pools accounting for respiration and mortality of phytoplankton. An offset phy_0 is included in the formulation of the linear losses to ensure that the phytoplankton concentration does not drop below the background concentration phy_0.

The sources and sinks of the diazotrophic phytoplankton are given by

$$\mathrm{sms}(\mathrm{nif})=\mu_{\mathrm{nif}}(\mathrm{dip},E,T,|\tau|)\mathrm{nif}-L_{\mathrm{nif,din}}\mathrm{nif}^2-L_{\mathrm{nif,det}}(\mathrm{nif}-\mathrm{nif}_0). \tag{5}$$

The diazotrophic growth rate μ_{nif} depends on the concentration of dip, the availability of photosynthetically active light $F_{\mathrm{nif}}(E)$ and the water temperature T and wind stress τ. The growth rate is defined as

$$\mu_{\mathrm{nif}}(\mathrm{dip},E,T,|\tau|)=F_{\mathrm{nif}}(E)\frac{\mathrm{dip}}{k_{\mathrm{P2}}+\mathrm{dip}}\,\mathrm{ampl}(T,|\tau|). \tag{6}$$

The photosynthesis–light relationship $F_{\mathrm{nif}}(E)$ is defined in analogy to Eq. (4) for phytoplankton as

$$F_{\mathrm{nif}}(E)=\frac{\mu_{\mathrm{nif}}^{\max}\alpha_2 E}{\sqrt{(\mu_{\mathrm{nif}}^{\max})^2+(\alpha_2 E)^2}}, \tag{7}$$

where $\mu_{\mathrm{nif}}^{\max}$ and α_2 are the maximum growth rate for the diazotrophs and their PI-initial slope, respectively. Diazotrophic growth rates are observed to increase during periods of high temperatures, low winds and calm seas (Carpenter, 1983; Carpenter and Capone, 1992; Karl et al., 1992; Wasmund, 1997). To account for this increase during favorable conditions we included a temperature- and wind-stress-dependent amplification factor ampl, defined as

$$\mathrm{ampl}(T,|\tau|)=\begin{cases}\frac{1}{3}(\tanh(2(T-T_{\mathrm{crit}}))+1)+\frac{1}{3} & \text{if } |\tau|\leqslant\tau_{\mathrm{crit}},\\ \frac{1}{6}(\tanh(2(T-T_{\mathrm{crit}}))+1)+\frac{1}{6} & \text{if } |\tau|>\tau_{\mathrm{crit}},\end{cases} \tag{8}$$

where T is the water temperature, $|\tau|$ the surface wind stress, and T_{crit} and τ_{crit} critical values for temperature and wind stress, respectively. Since doubling times of *Trichodesmium* are slow for

water temperatures between 20°C and 24°C (Mague et al., 1977; McCarthy and Carpenter, 1979; Carpenter et al., 1987) and maximal between 25°C and 30°C (Carpenter and Capone, 1992; Carpenter and Romans, 1991; Carpenter, 1983; Carpenter et al., 1987) the temperature dependence is defined such that growth rates gradually increase for temperatures between 24.5°C and 25.5°C (Fig. 2). The effect of wind speed on N_2 fixation rates, which has been reported by Bryceson and Fay (1981); Carpenter and Price (1977) and Wasmund (1997), is taken into account by a conditional statement that yields higher growth rates below the critical value for the surface wind stress τ_{crit}. Since no quantitative information about the effect of wind stress on the growth rate is available we have assumed doubling the growth rate below the critical values for the wind stress. The employed value for the critical wind stress corresponds to a wind velocity of 6 m s^{-1} as reported by Wasmund (1997). The respiration of the diazotrophs is assumed to depend quadratically on diazotrophic biomass to account for the observed high release rates of inorganic nitrogen during *Trichodesmium* blooms (Letelier and Karl, 1996). A background concentration nif_0 is included in the formulation of the mortality rate.

The zooplankton dynamics are determined by

$$\mathrm{sms(zoo)} = \gamma\mu_{\mathrm{zoo}}(\mathrm{phy})\mathrm{zoo} - L_{\mathrm{zoo,din}}(\mathrm{zoo} - \mathrm{zoo}_0) - L_{\mathrm{zoo,det}}\mathrm{zoo}^2. \tag{9}$$

The phytoplankton ingestion by zooplankton is parameterized as an s-shaped, quadratic Michaelis–Menten response

$$\mu_{\mathrm{zoo}}(\mathrm{phy}) = \mu_{\mathrm{zoo}}^{\max}\frac{\mathrm{phy}^2}{k_{\mathrm{phy}} + \mathrm{phy}^2}. \tag{10}$$

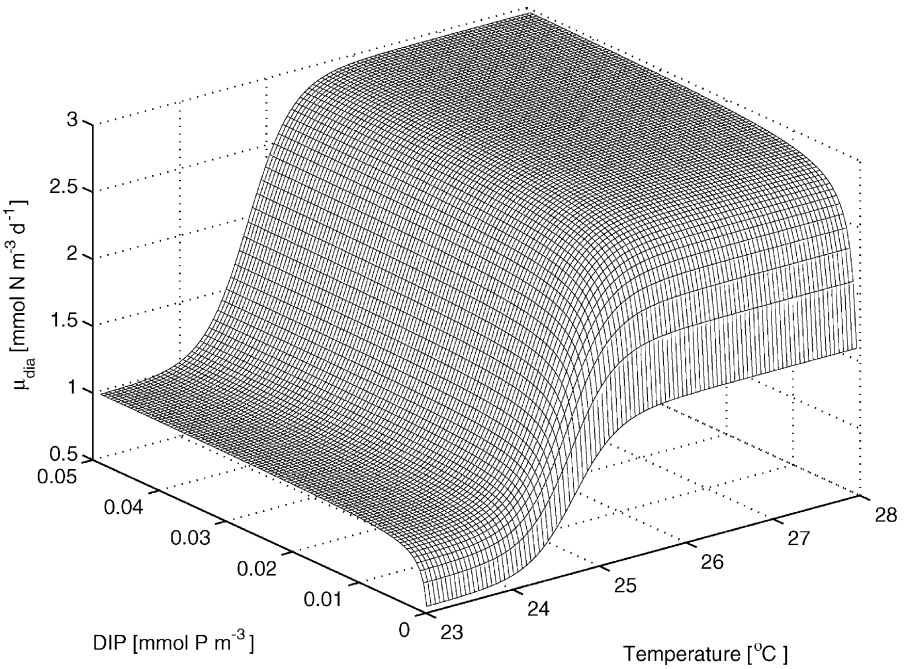


Fig. 2. The growth rate of diazotrophs as a function of temperature and dissolved inorganic phosphorus concentration.

Metabolic losses due to exudation enter the dissolved inorganic nutrient pools at a linear rate with the background concentration zoo_0, while zooplankton mortality is assumed to be quadratic.

The sources and sinks of the din and dip pools are written as

$$\begin{aligned}\mathrm{sms(din)} = & -\mu_{\mathrm{phy}}(\mathrm{din},\mathrm{dip},E)\mathrm{phy} + L_{\mathrm{phy,din}}(\mathrm{phy}-\mathrm{phy}_0) + L_{\mathrm{nif,din}}\,\mathrm{nif}^2 \\ & + L_{\mathrm{zoo,din}}(\mathrm{zoo}-\mathrm{zoo}_0) + \mathrm{rem}\,\mathrm{det}_N \end{aligned} \tag{11}$$

and

$$\begin{aligned}\mathrm{sms(dip)} = & -\frac{1}{r_1}\mu_{\mathrm{phy}}(\mathrm{din},\mathrm{dip},E)\mathrm{phy} - \frac{1}{r_2}\mu_{\mathrm{nif}}(\mathrm{dip},\varepsilon,T,\tau)\mathrm{nif} + \frac{1}{r_1}L_{\mathrm{phy,din}}(\mathrm{phy}-\mathrm{phy}_0) \\ & + \frac{1}{r_2}L_{\mathrm{nif,din}}\,\mathrm{nif}^2 + \frac{1}{r_1}L_{\mathrm{zoo,din}}(\mathrm{zoo}-\mathrm{zoo}_0) + \mathrm{rem}\,\mathrm{det}_{\mathrm{P}}, \end{aligned} \tag{12}$$

where r_1 and r_2 represent the cellular nitrogen to phosphorus ratios of phyto- and zooplankton and diazotrophs, respectively. r_2 is set to 45, which is a typical value for *Trichodesmium* (Letelier and Karl, 1996).

The time rates of change of the detrital pools are given as

$$\begin{aligned}\mathrm{sms}(\mathrm{det_N}) = & L_{\mathrm{phy,det}}(\mathrm{phy}-\mathrm{phy}_0) + L_{\mathrm{nif,det}}(\mathrm{nif}-\mathrm{nif}_0) \\ & + (1-\gamma)\mu_{\mathrm{zoo}}(\mathrm{phy})\mathrm{zoo} + L_{\mathrm{zoo,det}}\mathrm{zoo}^2 \\ & - \mathrm{rem}\,\mathrm{det_N} - w_{\mathrm{det}}\frac{\partial}{\partial z}\mathrm{det_N} \end{aligned} \tag{13}$$

and

$$\begin{aligned}\mathrm{sms}(\mathrm{det_P}) = & \frac{1}{r_1}L_{\mathrm{phy,det}}(\mathrm{phy}-\mathrm{phy}_0) + \frac{1}{r_2}L_{\mathrm{nif,det}}(\mathrm{nif}-\mathrm{nif}_0) \\ & + \frac{1}{r_1}(1-\gamma)\mu_{\mathrm{zoo}}(\mathrm{phy})\mathrm{zoo} + \frac{1}{r_1}L_{\mathrm{zoo,det}}\mathrm{zoo}^2 \\ & - \mathrm{rem}\,\mathrm{det_P} - w_{\mathrm{det}}\frac{\partial}{\partial z}\mathrm{det_P}. \end{aligned} \tag{14}$$

The particulate detrital material is assumed to sink at a constant velocity w_{det} of 2.5 m d^{-1}. The remineralization rate rem is chosen to be 0.01 d^{-1}. These parameter choices yield a value of 0.004 m^{-1} for the inverse of the solubilization length scale which is defined as $a = \mathrm{rem}/w_{\mathrm{det}}$. This is in agreement with the solubilization length scales for nitrogen and phosphorus estimated for sinking particles at the HOT site (Christian et al., 1997).

3.4. Model setup

The model is set up on a uniform grid covering the upper 350 m of the water column with a 5 m resolution. It is forced with daily values of the wind stress and the sensible, latent and downward short-wave components of the heat flux from the National Center for Environmental Prediction (NCEP) reanalysis data set. A typical albedo of 0.04 (Payne, 1972) was employed for the short-wave component. The lower boundary of the model domain is open to allow diffusive fluxes and sinking particles to cross the base of the model. The values of scalars and velocities are fixed at the base of the model, which implies a diffusive flux of din and dip into the domain, determined by the

background diffusion coefficient K_{back} (see Section 3.1) and the concentration gradients of din and dip. The initial conditions for temperature and salinity are interpolated from the profiles measured on January, 8 1989 at stn. ALOHA. The initial conditions for the biological variables are obtained from a one-year spin-up run. The spin-up run was initialized with nitrate + nitrite and phosphate profiles measured on January, 8 1989, where nitrite + nitrate corresponds to din and phosphate to dip. The other variables were set vertically constant to the background values shown in Table 1.

We applied a restoration of temperature to the monthly observed profiles, with a restoration time scale of 40 d. A comparison of observed and simulated temperatures with and without restoration is shown in Fig. 3. The simulation without restoration results in differences of up to 1°C to the observations in particular in 1990, early 1991 and 1992. The discrepancy may be due to unresolved advection of heat or errors in the surface forcing data. The restoration of model temperatures to the observed profiles corrects for the deviation and results in simulated temperatures that follow the observed profiles satisfactorily (Fig. 3).

We obtained estimates of the mixed-layer depth from the observed and simulated density profiles defining the depth of the mixed layer to be where the gradient of σ_t exceeds 1×10^{-4} kg m^{-4}. The simulated course of the mixed-layer depth compares well with the observed mixed-layer depths (Fig. 4).

4. Discussion of the model results

The euphotic zone in the oligotrophic subtropical North Pacific Ocean is characterized by low nutrient concentrations and low standing stocks of living organisms. A deep chlorophyll maximum layer (DCML) persists between 100 and 125 m, while chlorophyll concentrations in the upper euphotic zone are low. The mixed-layer depth at stn. ALOHA varies seasonally between 30 and 100 m. As the nutricline is located below 100 m (Dore and Karl, 1996), the deep mixing events in winter usually do not reach the nutricline, hence, there is no efficient entrainment of new nutrients into the euphotic zone. The simulated evolution of the mixed-layer depth and the inorganic nutrient profiles (Fig. 5) illustrate this year round oligotrophy. The simulated course of the diazotrophs and the other phytoplankton, and the detrital pools are shown in Figs. 6 and 7, respectively.

4.1. Chlorophyll

A comparison of simulated phytoplankton and observed chlorophyll concentrations is not straightforward since the euphotic zone at stn. ALOHA is characterized by two opposing seasonal cycles in its upper and lower parts and by varying carbon to chlorophyll (C : chl) ratios of the phytoplankton community. The euphotic zone has been described as a two-layer system. The upper part (0–50 m) is characterized by a quasi-steady-state cycling of regenerated nutrients and little seasonality (Letelier et al., 1993; Winn et al., 1995). Primary production in the upper euphotic zone is high throughout the year with very low new production (Karl et al., 1996). An observed recurring increase of chlorophyll concentrations in winter has been attributed to photoadaption. Since mixing depths increase in winter the nutrient-limited phytoplankton

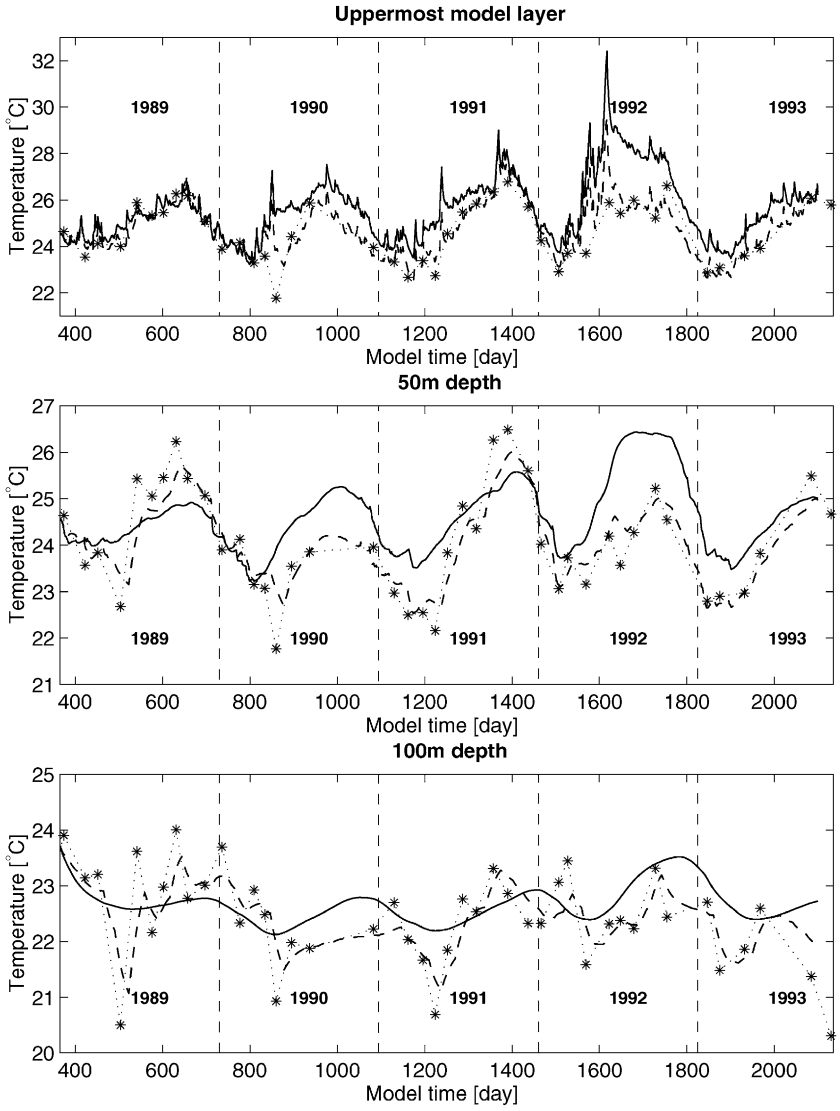


Fig. 3. Simulated and observed temperatures at the surface (upper), 50 m depth (middle) and 100 m depth (lower panel). The solid line indicates the predicted temperatures without restoration to observations (asterisks) while the dashed line represents the temperature predicted with restoration to the measurements.

community compensates for lower light levels by an increase in cellular chlorophyll content without an associated increase in biomass (Letelier et al., 1993; Winn et al., 1995). The lower part of the euphotic zone (100–175 m) displays an opposing seasonal cycle with increasing chlorophyll concentrations in spring. The primary production rates in the lower euphotic zone are small in winter and increase in spring with maximum values in late spring. This spring chlorophyll increase is associated with net growth and accumulation of autotrophic biomass. Since the phytoplankton

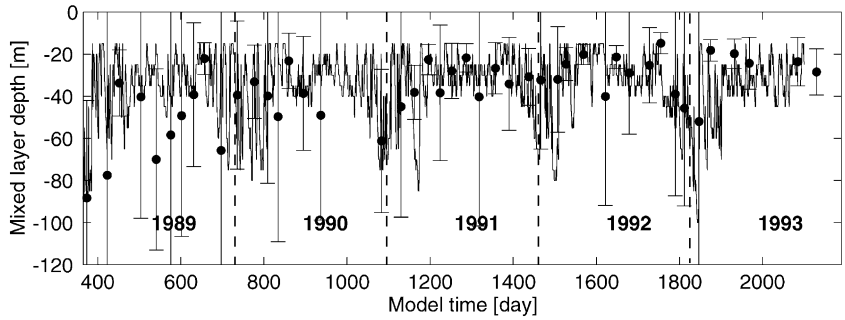


Fig. 4. Model-predicted and observed mixed-layer depths at stn. ALOHA. The measured values are presented as mean mixed-layer depth values ± 1 standard deviation of the means as determined from multiple (generally 15) CTD casts on each cruise.

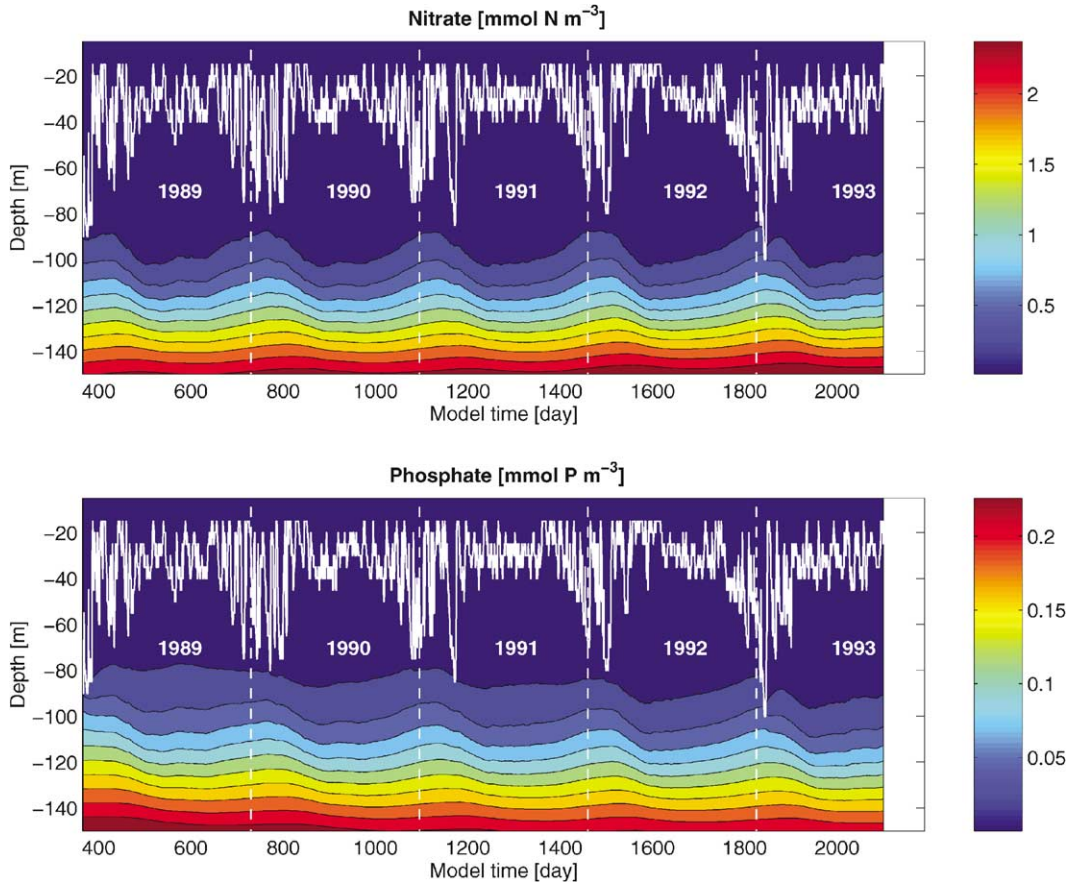


Fig. 5. Simulated nitrate and phosphate concentrations. The mixed-layer depth is indicated by the white line.

community in the lower part of the euphotic zone is light-limited the C : chl ratio shows only little variation. Changes in chlorophyll concentration there correspond more likely to changes in phytoplankton biomass than in the upper euphotic zone.

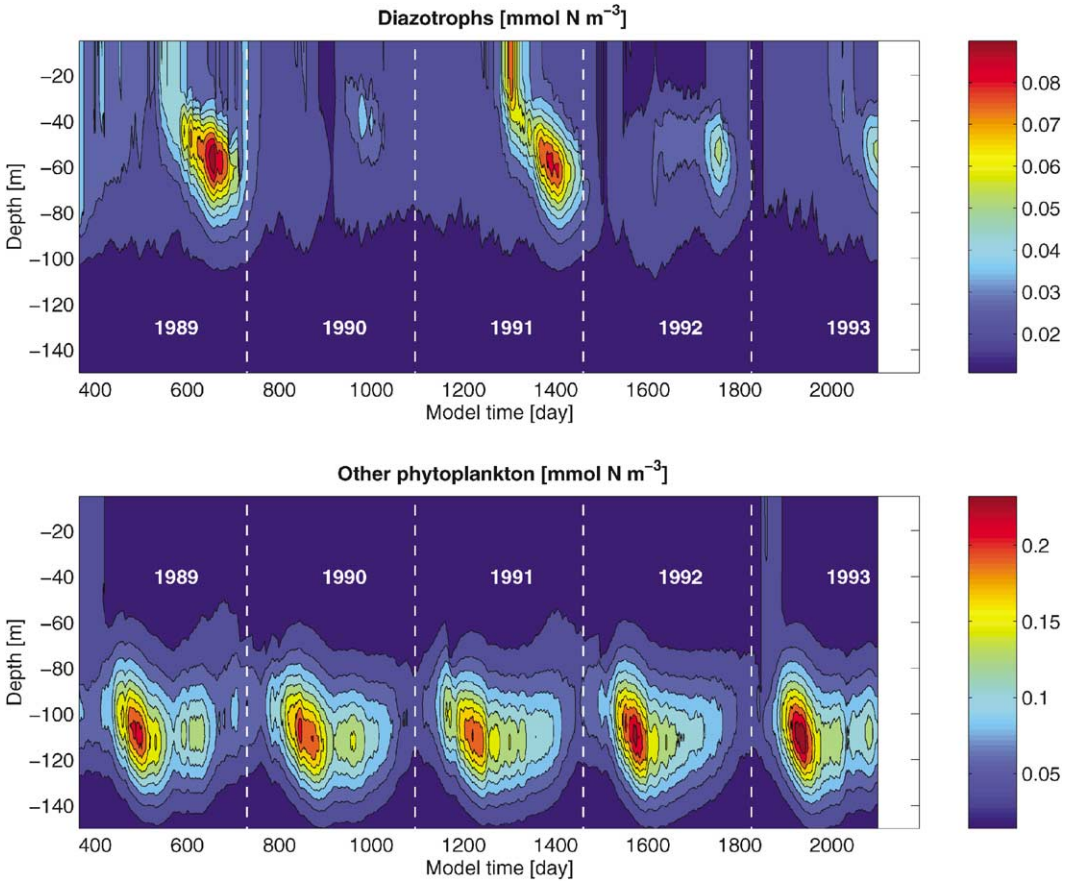


Fig. 6. Simulated biomass of the diazotrophs and the other phytoplankton.

To compare model-predicted and observed chlorophyll concentrations, the two-layer structure of the euphotic zone with its opposing seasonal cycles has to be taken into account. We calculated the mean chlorophyll concentrations for the simulated and measured profiles for both parts of the euphotic zone employing a constant mean C : chl ratio of 50 g : g to convert the simulated biomass. In the upper part of the euphotic zone the magnitude of observed and simulated chlorophyll compares well for most of the spring and summer values (Fig. 8, upper panel). As we would expect, the slightly elevated chlorophyll concentrations in winter are generally underestimated by the model, since this winter increase is due to photoadaption which is not accounted for in the model. In the lower euphotic zone the magnitude and course of the simulated and observed chlorophyll values compare well. The simulated concentrations lie within the range of standard deviation for almost all measured values (Fig 8, middle panel). Since the vertical integration is performed over a greater depth range than the actual deep chlorophyll maximum, the standard deviations are relatively high. The location of the DCML is known to show a seasonal vertical displacement of about 20 m (Letelier et al., 1996), following the seasonal variation of the isolumes. As an attempt to decrease the standard deviation for the comparison we calculated the vertical means over the depth range defined by the 5 and 1 W m^{-2} isolumes of the simulated

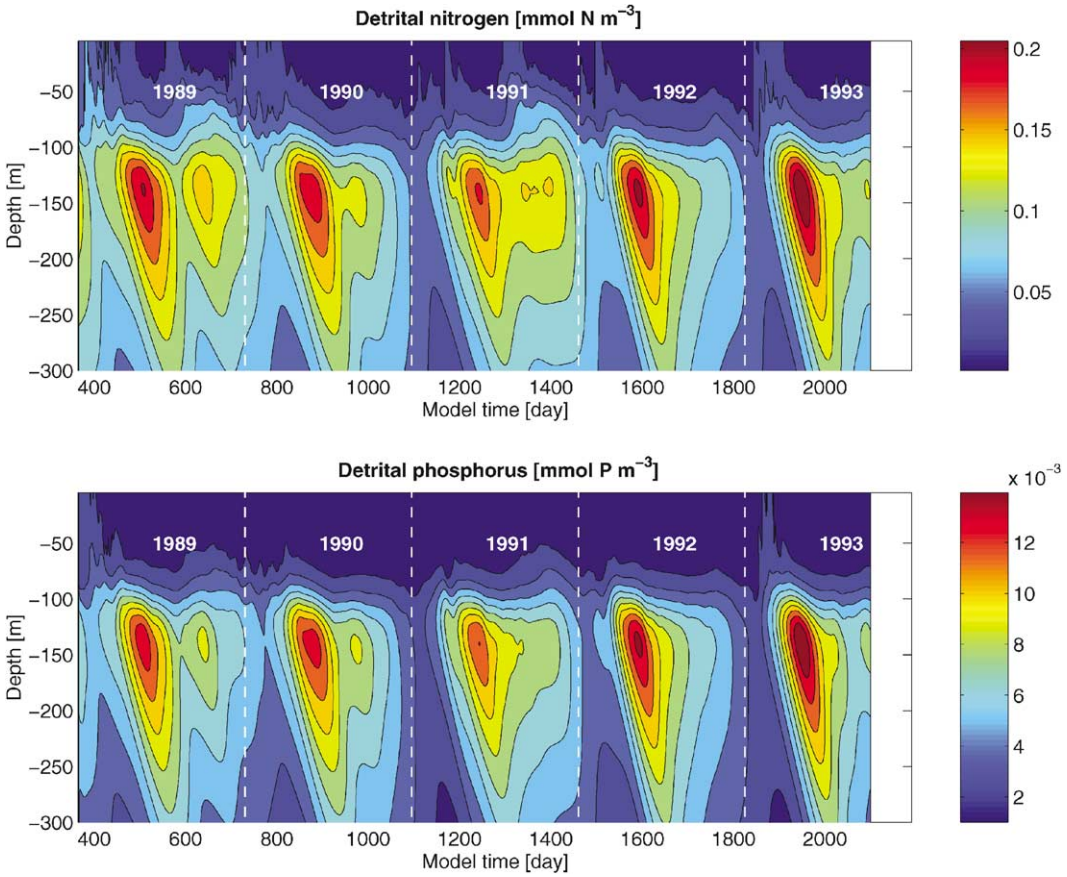


Fig. 7. Simulated detrital nitrogen and phosphorus concentrations.

photosynthetically active radiation. This restricts the vertical integration closer to the actual DCML. The simulated magnitude and course of the chlorophyll concentrations in the DCML are in good agreement with the corresponding observed values (Fig. 8, lower panel).

4.2. *Vertical particle fluxes and inorganic nutrient concentrations*

Observed vertical particle fluxes at stn. ALOHA vary considerably without a consistent seasonal pattern and are dominated by stochastic export events, thus most likely are subject to undersampling by a monthly sampling frequency (Karl et al., 1996). The variability in particle export is believed to be the result of sporadic nutrient injections that are driven by intermittent physical mechanisms like internal waves, mesoscale eddies, wind-driven Ekman pumping and atmospheric storms (Karl, 1999). The sporadic nutrient injections represent an important input of new nutrients into the euphotic zone, thus contributing significantly to export production. Since the model does not resolve the sporadic physical events, vertical eddy diffusion is the only mechanism in the model to bring new nutrients from below into the euphotic zone, the particle

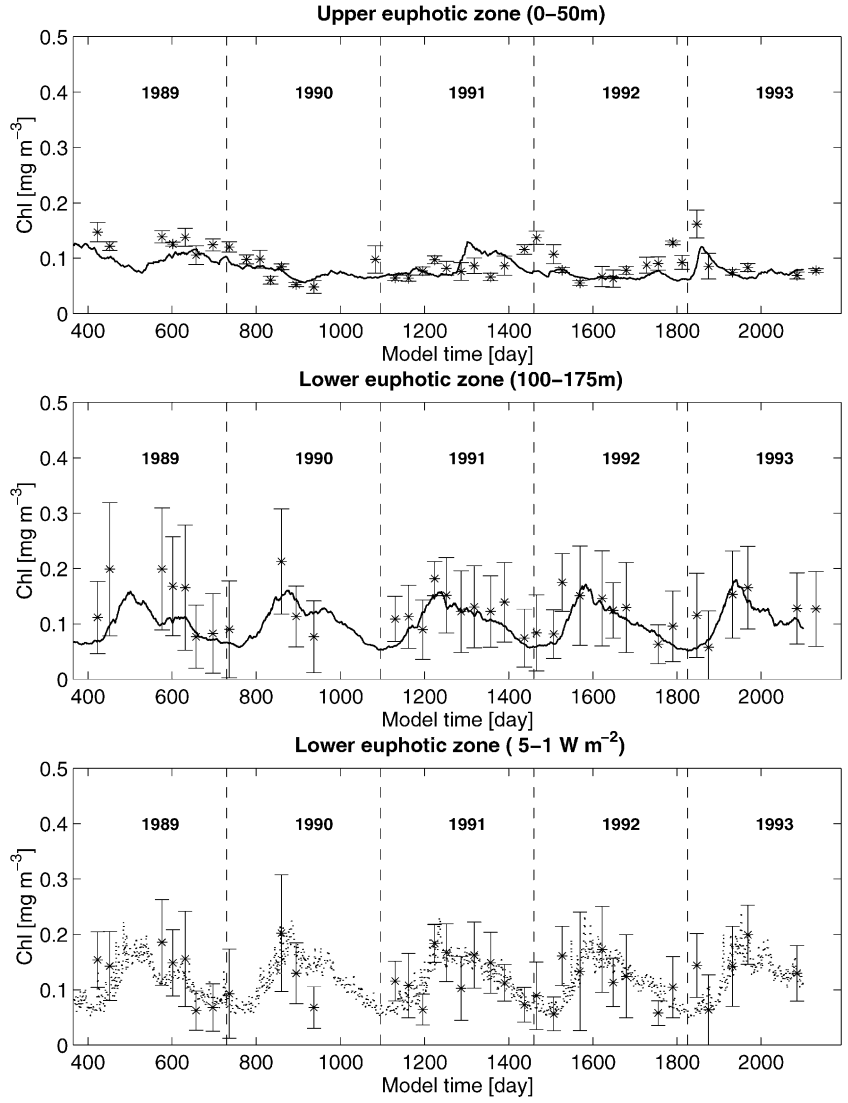


Fig. 8. Simulated and observed chlorophyll concentrations in the upper and lower euphotic zone. The model predicted chlorophyll was obtained by converting the biomass of diazotrophs and the other phytoplankton assuming a constant mean C : chl ratio of 50 g : g. Vertical means shown in the lower panel were calculated over the depth range defined by the 1 and 5 W m^{-2} isolines of the predicted photosynthetically active radiation.

export predicted by the model (Fig. 9) is lacking any high amplitude export events. However, the magnitude of simulated and observed fluxes compares well, especially during the period from 1989 to 1991, while export rates in 1992 and 1993 are overestimated. The model predicted export in 150 m depth (Fig. 10, upper panel) is in good agreement with the estimated mean value of particle export of 0.28 ± 0.11 mmol N m^{-2} d^{-1} for the period from 1988 to 1994 (Christian et al., 1997). The yearly integrated values of simulated and observed export fluxes at 150 and at 300 m agree well in particular in 1989, 1990 and 1991 (Fig. 10, lower panel).

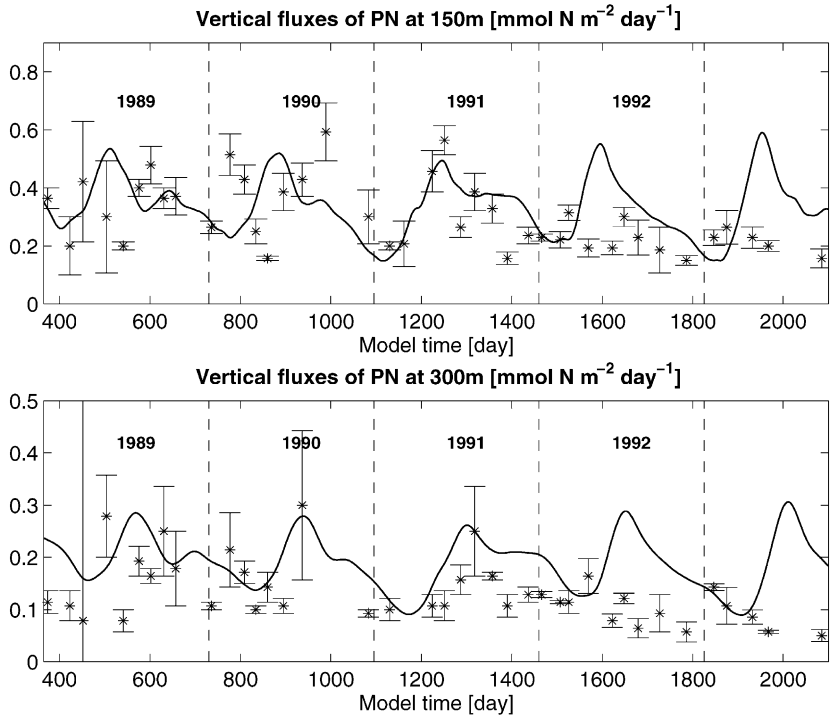


Fig. 9. Model-predicted and observed vertical fluxes of particulate nitrogen (PN) at 150 and 300 m depth (upper and lower panel, respectively) with error bars representing the standard deviation of the measurements.

The pools of inorganic nutrients in the model change gradually over time (Fig. 11). The model is not capable of simulating the observed short-term fluctuations since the steady-state eddy diffusive flux is the only mechanism to bring nutrients from below into the euphotic zone. The short-term changes in measured inorganic nutrient pools at stn. ALOHA can be attributed to sporadic vertical mixing events and horizontal advective transport by passing mesoscale eddies, both not captured in the model. The predicted mean values of din in the upper 150 m of the water column are continuously higher than the observed values of nitrate + nitrite (Fig. 11, upper panel), while the mean values of the simulated dip slightly underestimate the data (Fig. 11, lower panel). A decreasing trend in dip over the 5-year simulation period is present in the model results as well as in the observed data.

In regard to the overestimated din concentrations it has to be noted, that the simulated din comprises all inorganic nutrient compounds including ammonium while the measured values represent nitrate and nitrite only. Ammonium concentrations are generally assumed to be low. However, during *Trichodesmium* blooms values of up to 1.6 mmol NH_4^+ m^{-3} have been observed (Karl et al., 1992). Furthermore, the model does not account for any dissolved organic nitrogen, which is present in relatively high concentrations in the upper 100 m at stn. ALOHA. The dynamics of the microbial loop and bacterial remineralization of dissolved organic matter are only included indirectly by direct fluxes from the plankton and detrital pools to dissolved inorganic nutrients. This simplistic treatment of the microbial processes might contribute to the

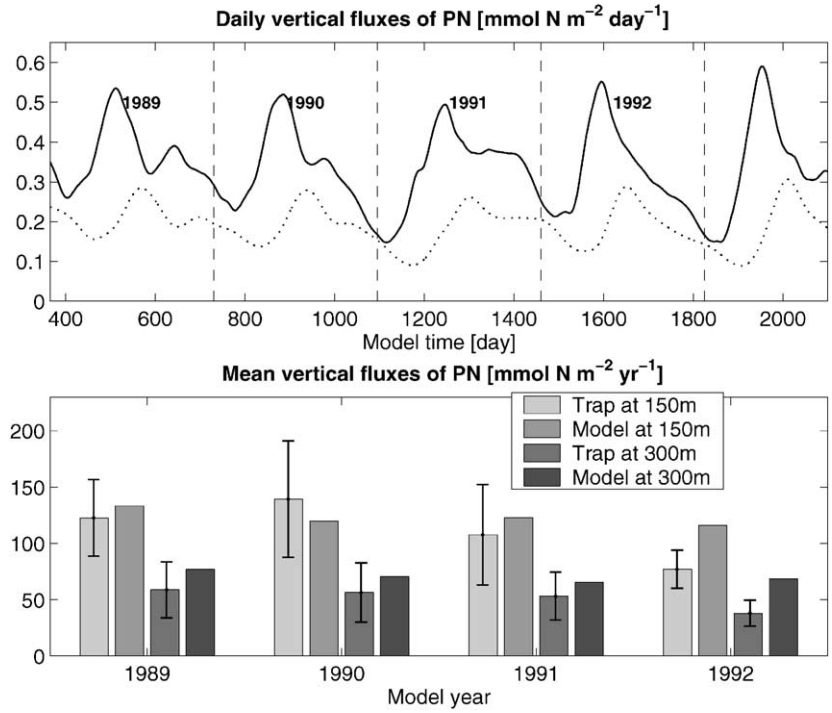


Fig. 10. Model-predicted vertical fluxes of particulate nitrogen (PN) at 150 m (solid) and 300 m depth (dashed line, upper panel). Comparison of observed and model-predicted yearly vertical fluxes of PN (lower panel) with error bars representing the standard deviation of the measurements.

discrepancy between the simulated and observed din pools. Furthermore, the sensitivity of the results to the choice of the biological model parameters has not been explored thoroughly. The use of data assimilation techniques for parameter optimization could help to calibrate the model parameters (Fennel et al., 2001; Spitz et al., 2001).

4.3. Seasonal cycle and interannual variability of diazotrophs

Observed concentrations of *Trichodesmium* at stn. ALOHA are highly variable, with averages over the upper 45 m of the water column ranging from 0.009 to 0.065 mmol N m^{-3} (Letelier and Karl, 1996; concentrations given in trichomes per m^3 were converted assuming additional 12% of *Trichodesmium* biomass in colonies and a mean nitrogen content of 9.5 ng per filament). *Trichodesmium* concentrations follow a seasonal cycle, with low cell numbers during winter and spring and highest concentrations at the end of summer. Considerable interannual variability was observed with an intense bloom in August 1989 compared to low abundances in 1990 and significantly higher concentrations in 1991 and 1992. The seasonal cycle as well as interannual differences are captured by the model (Fig. 6). A seasonal pattern with highest concentrations of up to 0.08 mmol N m^{-3} at the end of summer and lowest concentrations of 0.02 mmol N m^{-3} during winter and spring are predicted by the model. In late summer of 1989 a bloom of

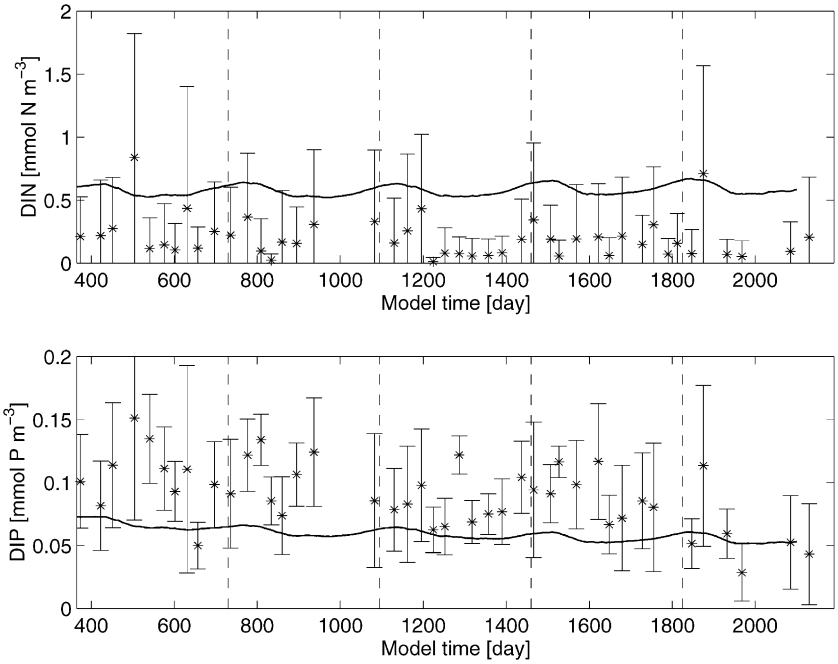


Fig. 11. Model-predicted and observed pools of dissolved inorganic nitrogen (upper panel) and phosphorus (lower panel) integrated over the upper 150 m of the water column with error bars representing the standard deviation of the measurements within the integration interval of the actual profile.

diazotrophs is simulated while diazotrophic biomass remains below 0.03 mmol N m^{-3} in 1990, which is in good agreement with the observed values of less than 0.031 mmol N m^{-3} throughout 1990. High diazotrophic concentrations with maximum values of 0.08 mmol N m^{-3} for late summer in 1991 and 0.05 mmol N m^{-3} in 1992 agree qualitatively with the observed maximum values of 0.062 mmol N m^{-3} for 1991 and 1992.

At stn. ALOHA, *Trichodesmium* is abundant only in the upper 80 m of the water column, with a subsurface maximum between 20 and 50 m depth (Letelier and Karl, 1996). The model simulates high concentrations of diazotrophs within the mixed layer only during the early phase of blooms, while later during their course maximum abundances occur between 40 and 80 m depth (Fig. 6, see esp. 1989 and 1990). This slight discrepancy between observed and simulated vertical structure can be attributed to the fact that *Trichodesmium* colonies migrate vertically, which is a feature unresolved by the model. *Trichodesmium* contains gas vacuoles that allow a positive buoyancy and have the ability to change its vertical position by the production and consumption of "ballast" carbohydrates. Since the model diazotrophs are not capable of vertical migration, their growth in the upper 40 m is impeded after the available dissolved inorganic phosphorus has been taken up. Furthermore, *Trichodesmium* utilizes phosphorus from the dissolved organic matter pool (Yentsch et al., 1972), which is not accounted for by the model. This difference in vertical distribution is taken into account when comparing observed and model predicted diazotrophs. The order-of-magnitude and the temporal course of observed *Trichodesmium* at stn. ALOHA with increasing abundances in 1991 and 1992 and relatively low values in 1990 agree well with the

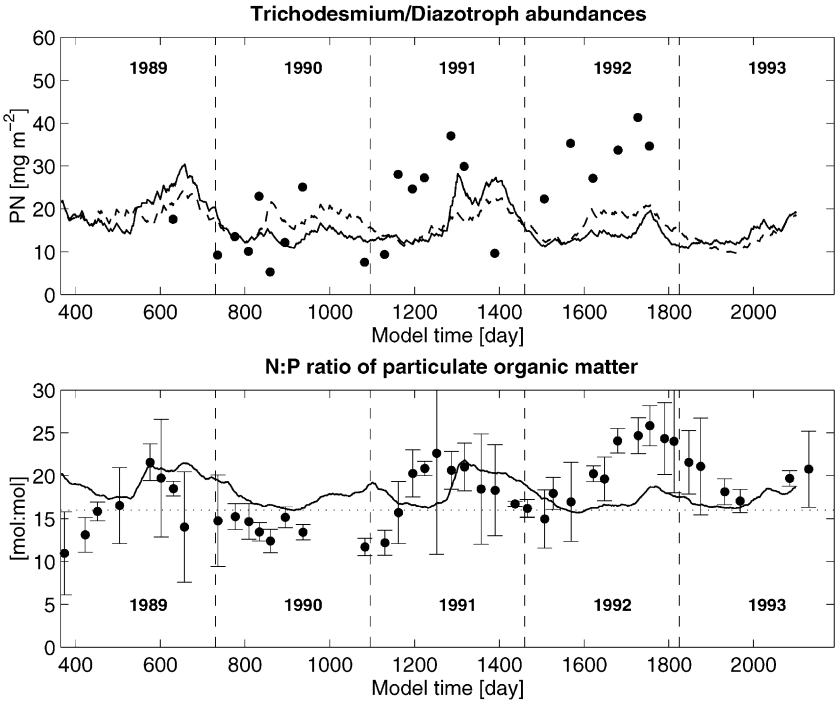


Fig. 12. Simulated and observed diazotroph abundances (upper panel). Measurements (filled dots) are integrated over the upper 45 m of the water-column while model concentrations represent the mean value over the upper 100 m integrated over 45 m. The solid line refers to the default simulation, while the dashed line is predicted by a model run without restoration of temperature. Simulated and observed N : P stoichiometry of particulate matter within the upper 100 m of the water-column (lower panel). The Redfield ratio value of 16 is indicated by the dotted horizontal line.

simulated diazotrophic biomasses in 1990 and 1991 (Fig. 12, upper panel). The simulated biomasses in 1992 are too low. A temporal pattern in the N : P ratio of suspended particles that coincides with the seasonal pattern of *Trichodesmium* abundances is observed at stn. ALOHA (Karl et al., 1997). The N : P ratios are substantially higher than the Redfield ratio during summer periods, with high *Trichodesmium* abundances and drop below the Redfield value during winter. The model predicted N : P ratio of particulate organic matter follows the observed temporal course qualitatively between 1989 and 1991, while the N : P ratios in 1992 are underestimated by the model (Fig. 12, lower panel).

To illustrate the simulated interannual differences of nitrogen fluxes, the yearly integrated fluxes between the different model pools are shown in Fig. 13. The model predicted N_2 fixation rates range from 26.7 to 54.3 mmol N m^{-2} yr^{-1}. These values lie within the range of values reported by Karl et al. (1997), who present estimates varying from 31 ± 18 to 51 ± 26 mmol N m^{-2} yr^{-1} based on a variety of different methods. In 1990 the simulated N_2 fixation rate is substantially lower than in 1989 and 1991, which can be attributed to the lower water temperatures in 1990. The phytoplankton uptake and losses show little interannual variability.

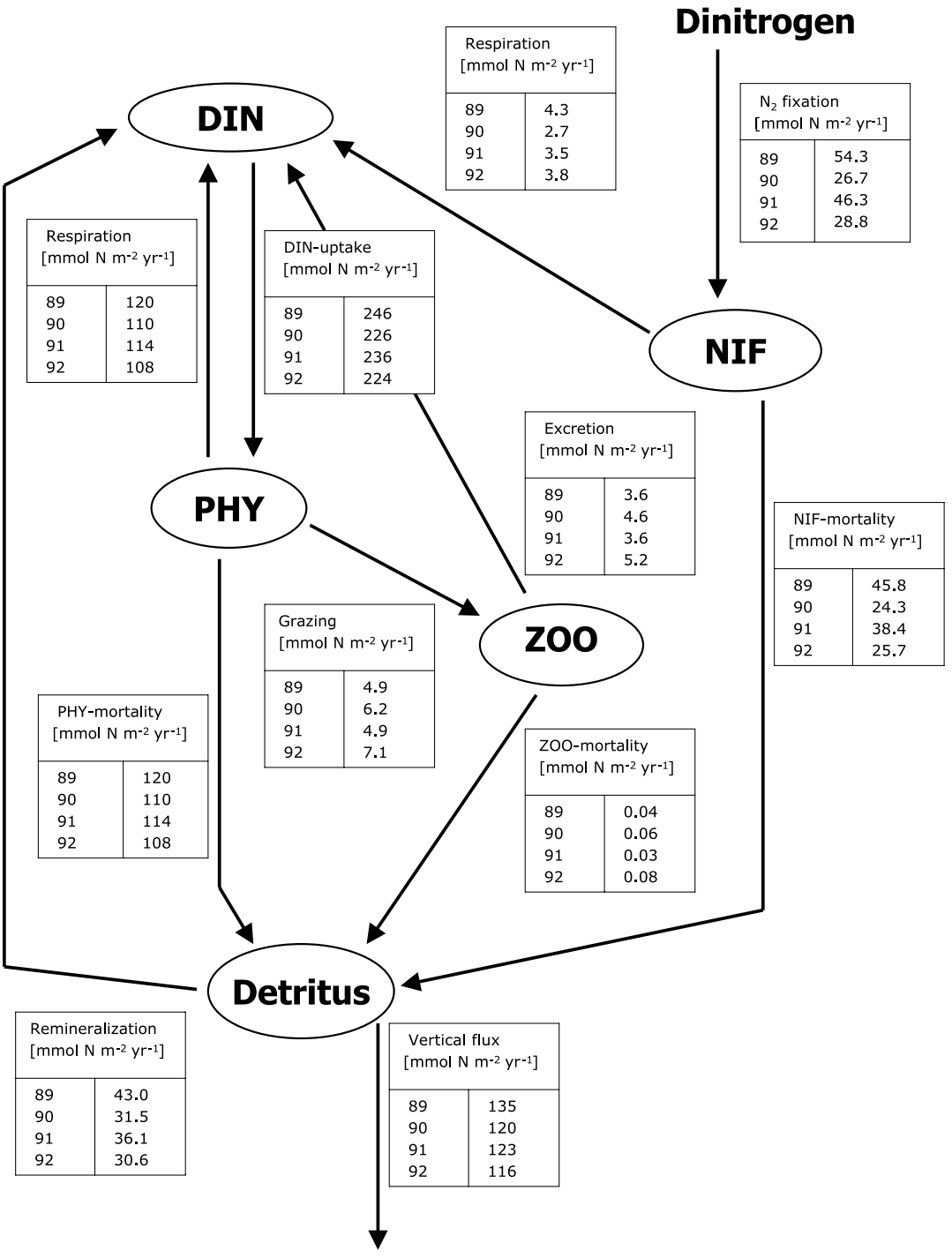


Fig. 13. Simulated yearly fluxes of nitrogen between the different model components. Values are integrated over the upper 150 m of the water column. The sinking flux is calculated at 150 m.

Table 3
Data-based and model-predicted yearly rates of N_2 fixation and vertical particle flux[a]

	N_2 fixation rates (mmol N m^{-2} yr^{-1})			
Data-based estimates	$31 \pm 18 \cdots 51 \pm 26$			
Year	1989	1990	1991	1992
Default run	54.3	26.7	46.3	28.8
No restoration	48.4	38.5	39.6	39.5
	Vertical flux of PN at 150 m (mmol N m^{-2} yr^{-1})			
Data-based estimates	$77 \pm 17 \cdots 139 \pm 52$			
Year	1989	1990	1991	1992
Default run	134.8	119.8	123.4	115.6
No restoration	131.8	125.5	122.4	121.7

[a] The default run refers to the simulation with temperature restoration to observed profiles. The data-based estimates for the yearly N_2 fixation follow Karl et al. (1997), while the vertical flux estimates represent the range of the yearly integrated fluxes calculated from the HOT data set.

4.4. Sensitivity to temperature

The biological component of a coupled physical/biological model can only be expected to give reasonable results if the essential physical processes are simulated correctly. This holds especially true if physical properties like temperature enter the biological parameterizations. In the present model the N_2 fixation rate is directly dependent on temperature. As described in Section 3.3, fixation rates increase if the temperature exceeds a critical value. The default simulation described above employs a temperature restoration to obtain temperature predictions that match the observed values as closely as possible. However, such restorations are only practical if a data set with sufficient temporal resolution is available and are less feasible in a three-dimensional context. To investigate how the model results depend on the simulated temperatures a model simulation of the coupled model without temperature restoration was performed in comparison to the default simulation. The simulated temperatures differ mainly in 1990, 1991 and 1992 by about 1°C. In 1992 the simulated temperature without restoration is about 2°C too high during spring and summer (Fig. 3).

The simulation without restoration predicts yearly values of N_2 fixation and particle export that are within the range of data-based estimates (Table 3), but the interannual pattern did change. The temperature deviation in 1990 and early 1992 results in an increase of N_2 fixation and diazotrophic biomass (Fig. 12, upper panel). The yearly N_2 fixation increased by 44% in 1990 compared to the default simulation (Table 3). The other phytoplankton show no significant response to the higher N_2 fixation but the particle export increased by 5% in 1990 and 1992 (Table 3).

5. Summary

We have presented a relatively simple biological model of an oligotrophic system that includes a mechanistically-based description of N_2 fixation by diazotrophic phytoplankton and resolves the

uncoupled elemental cycling of nitrogen and phosphorus in the euphotic zone. The mechanistic parameterization for N_2 fixation is based on physiological responses of *Trichodesmium* to the physical conditions of their environment. This model is meant as a step towards a more realistic inclusion of the supply of new nitrogen to the marine nitrogen cycle through N_2 fixation and varying elemental stoichiometries in nutrient fluxes into coupled biogeochemical models.

A model simulation at stn. ALOHA in the North Pacific Subtropical Gyre reproduces essential features of the biological system including the vertical structure and seasonal variations in chlorophyll, the seasonal cycle and interannual differences in the occurrence of diazotrophs, the seasonal variations in N : P stoichiometries of organic matter, the mean flux of particulate matter out of the euphotic zone, and a drift in the relative importance of nitrogen versus phosphorus control of the phytoplankton community. Current limitations of the model include the overestimation of the dissolved inorganic nitrogen concentrations in the euphotic zone and the implicit treatment of the microbial loop. Also, it has to be noted that the parameterization for N_2 fixation is sensitive to temperature variations in the critical range between 24°C and 25°C. An exact prediction of temperature by the physical model component is thus crucial for the representation of N_2 fixation.

Although N_2 fixation has been recognized as a key process in biogeochemical cycling and might directly affect atmospheric CO_2 concentrations (Falkowski, 1997), this process is not adequately accounted for in current biogeochemical models. Until recently biogeochemical modeling studies to assess and predict the ocean's role in the global carbon cycle have been using a "static" approach, based on the cycling of a single element (N or P), to account for the biologically mediated export of carbon. Feedback mechanisms that change the supply rate of new nutrients, like N_2 fixation, and variations in elemental stoichiometries with shifts in community structure are two of the four basic mechanisms that can change the efficiency of the biological pump, the others being changes in the form of organic carbon produced, and changes in the ratio of organic carbon to calcium carbonate (OCTET Report, 2000). Their inclusion into biogeochemical models is crucial to understanding the role of the biological pump in the marine carbon cycle. We demonstrate in this study that a deterministic inclusion of feedback mechanisms, in particular N_2 fixation and variations in elemental stoichiometries, into simple biogeochemical models is feasible.

We did not attempt to include a microbial community, since a deterministic description of the complex nutrient dynamics associated with the DOM pools requires a mechanistic understanding of the inventories and fluxes of nitrogen and phosphorus. At this stage a comprehensive concept of these complex dynamics and its consequences for biogeochemical cycling is lacking. Crucial questions that remain to be addressed include the identification of the labile and refractory fractions of DOM pools, explanation of the significant differences in molar stoichiometries of dissolved organic nutrient pools compared to the pools of inorganic nutrients (Karl et al., 2001b), and the higher "resistance" of DON to microbial recycling compared to DOP, which implies a differential transfer of DON and DOP to refractory compounds (Wu et al., 2000).

An analysis of the sensitivity of our model results to the N : P ratio of diazotrophic uptake remains to be done. We assumed a N : P ratio of 45, which represents the mean value observed at stn. ALOHA over the period from October 1989 to December 1992 (Letelier and Karl, 1996), although during intense *Trichodesmium* blooms N : P ratios of up to 125 have been observed (Karl

and Karl et al., 1992). Higher N : P ratios for diazotrophic growth would probably lead to enhanced phosphorus limitation in the euphotic zone.

We did not account for the potential regulation of phytoplankton production by iron and the potential iron limitation of the diazotrophs, but recent results suggest that iron supply may be a limiting factor at stn. ALOHA (Wu et al., 2001). However, iron is likely to regulate the phytoplankton growth rate and biomass in the equatorial region of the Pacific (Landry et al., 1997) and may play an important role in regulating diazotrophic growth. N_2 fixation is an iron-intensive metabolic process compared to the assimilation of fixed forms of nitrogen, since nitrogenase, the enzyme for nitrogen fixation, has a high iron content (Rueter et al., 1990, 1992; Paerl et al., 1994). Other issues to be explored in the future are the vertical migration of *Trichodesmium* colonies, which allows an incorporation of inorganic phosphorus from greater depths (Karl et al., 1992; Letelier and Karl, 1998) and the utilization of dissolved organic phosphorus (Yentsch et al., 1972).

Acknowledgements

We thank Jim Richman for helpful discussions and appreciate the thoughtful comments from Scott Doney, Keith Moore and 2 anonymous reviewers. This work has been supported by a grant from the National Aeronautics and Space Administration (NAG5-4947). US JGOFS contribution No. 617.

References

Azam, F., 1998. Microbial control of oceanic carbon flux: the plot thickens. Science 280, 694–696.

Bissett, W.P., Walsh, J.J., Dieterle, D.A., Carder, K.L., 1999. Carbon cycling in the upper waters of the Sargasso Sea: I. Numerical simulation of differential carbon and nitrogen fluxes. Deep-Sea Research I 46, 205–269.

Brock, T.D., 1981. Calculating solar radiation for ecological studies. Ecological Modelling 14, 1–19.

Bryceson, I., Fay, P., 1981. Nitrogen fixation in *Oscillatoria* (*Trichodesmium*) *erythraea* in relation to bundle formation and trichome differentiation. Marine Biology 61, 159–166.

Capone, D.G., Carpenter, E.J., 1999. Nitrogen fixation by planktonic cyanobacteria: historical and global perspectives. Symposium on Marine Cyanobacteria. Bull. Inst. Oceanography, Vol. 19, Monaco, pp. 235–256.

Capone, D.G., Zehr, J.P., Paerl, H.W., Bergman, B., Carpenter, E.J., 1997. *Trichodesmium*, a globally significant marine cyanobacterium. Science 276, 1221–1229.

Capone, D.G., Subramaniam, A., Montoya, J.P., Voss, M., Humborg, C., Johansen, A.M., Siefert, R.L., Carpenter, E.J., 1998. An extensive bloom of the N_2-fixing cyanobacterium *Trichodesmium erythraeum* in the central Arabian Sea. Marine Ecology Progress Series 172, 281–292.

Carpenter, E.J., 1983. Physiology and ecology of marine planktonic *Oscillatoria* (*Trichodesmium*). Marine Biology Letters 4, 69–85.

Carpenter, E.J., Capone, D.G., 1992. Nitrogen fixation in *Trichodesmium* blooms. In: Carpenter, E.J., et al. (Ed.), Marine Pelagic Cyanobacteria: *Trichodesmium* and Other Diazotrophs. Kluwer Academic Publishers, Netherlands, pp. 211–217.

Carpenter, E.J., Price, C.C., 1977. Nitrogen fixation, disruption, and production of *Oscillatoria* (*Trichodesmium*) *spp*. in the western Sargasso and Caribbean Seas. Limnology and Oceanography 22, 60–72.

Carpenter, E.J., Romans, K., 1991. Major role of the cyanobacterium *Trichodesmium* in nutrient cycling in the North Atlantic Ocean. Science 254, 1356–1358.

Carpenter, E.J., Scranton, M.I., Novelli, P.C., Michaels, A., 1987. Validity of N_2 fixation rate measurements in marine *Oscillatoria* (*Trichodesmium*). Journal of Plankton Research 9, 1047–1056.

Christian, J.R., Lewis, M.R., Karl, D.M., 1997. Vertical fluxes of carbon, nitrogen and phosphorus in the North Pacific subtropical gyre. Journal of Geophysical Research 102, 15667–15677.

Codispoti, L.A., Berger, W.H., 1989. Phosphorus vs. nitrogen limitation of new and export production. In: Berger, et al. (Eds.), Productivity of the Ocean: Present and Past, Wiley, Berlin, pp. 377–394.

Doney, S.C., 1999. Major challenges confronting marine biogeochemical modeling. Global Biogeochemical Cycles 13, 705–714.

Doney, S.C., Glover, D.M., Najjar, R.G., 1996. A new coupled, one-dimensional model for the upper ocean: applications to the JGOFS Bermuda Atlantic Time-series Study (BATS) site. Deep-Sea Research II 43, 591–624.

Dore, J.E., Karl, D.M., 1996. Nitrite distributions and dynamics at Station ALOHA. Deep-Sea Research II 43, 385–402.

Duffie, J.A., Beckman, W.A., 1980. Solar Engineering of Thermal Processes. Wiley-Interscience, New York, p. 762.

Evans, G.T., Parslow, J.S., 1985. A model of annual plankton cycles. Biological Oceanography 3, 327–347.

Fasham, M.J.R., Ducklow, H.W., McKelvie, S.M., 1990. A nitrogen-based model of plankton dynamics in the oceanic mixed-layer. Journal of Marine Research 48, 591–639.

Falkowski, P.E., 1997. Evolution of the nitrogen cycle and its influence on the biological sequestration of CO_2 in the ocean. Nature 387, 272–275.

Fennel, K., Losch, M., Schröter, J., Wenzel, M., 2001. Testing a marine ecosystem model: sensitivity analysis and parameter optimization. Journal of Marine Systems 28, 45–63.

Hood, R.R., Michaels, A., Capone, D.G., 2000. Answers sought to the enigma of marine nitrogen fixation. EOS, Transactions of the American Geophysical Union 81, 133–139.

Hood, R.R., Bates, N.R., Capone, D.G., Olson, D.B., 2001. Modeling the effect of nitrogen fixation on carbon and nitrogen fluxes at BATS. Deep-Sea Research II 48, 1609–1648.

Kana, T.M., 1992. Oxygen cycling in cyanobacteria with specific reference to oxygen protection in *Trichodesmium* spp. In: Carpenter, E.J., et al. (Ed.), Marine Pelagic Cyanobacteria: *Trichodesmium* and Other Diazotrophs. Kluwer Academic Publishers, Netherlands, pp. 29–41.

Karl, D.M., 1999. A sea of change: Biogeochemical variability in the North Pacific subtropical gyre. Ecosystems 2, 181–214.

Karl, D.M., Lukas, R., 1996. The Hawaii Ocean Time-series (HOT) program: background, rationale and field implementation. Deep-Sea Research II 43, 129–156.

Karl, D.M., Letelier, R., Hebel, D.V., Bird, D.F., Winn, C.D., 1992. *Trichodesmium* blooms and new nitrogen in the North Pacific gyre. In: Carpenter, E.J., et al. (Ed.), Marine Pelagic Cyanobacteria: *Trichodesmium* and Other Diazotrophs. Kluwer Academic Publishers, Netherlands, pp. 219–237.

Karl, D.M., Christian, J.R., Dore, J.E., Hebel, D.V., Letelier, R.M., Tupas, L.M., Winn, C.D., 1996. Seasonal and interannual variability in primary production and particle flux at Station ALOHA. Deep-Sea Research II 43, 539–568.

Karl, D.M., Letelier, R., Tupas, L., Dore, J., Christian, J., Hebel, D., 1997. The role of nitrogen fixation in biogeochemical cycling in the subtropical North Pacific Ocean. Nature 388, 533–538.

Karl, D.M., Björkman, K.M., Dore, J.E., Fujieki, L., Hebel, D.V., Houlihan, T., Letelier, R.M., Tupas, L.M., 2001b. Ecological nitrogen-to-phosphorus stoichiometry at station ALOHA. Deep-Sea Research II 48, 1529–1566.

Karl, D.M., Michaels, A., Bergman, B., Capone, D.G., Carpenter, E., Letelier, R., Lipschultz, F., Paerl, H., Sigman, D., Stal, L., 2001a. Nitrogen fixation in the world's oceans. Biogeochemistry, in press.

Kraus, E.B., 1972. Atmosphere–Ocean Interaction, Clarendon Press, Oxford, UK, p. 275.

Landry, M.R., Barber, R.T., Bidigare, R.R., Chai, F., Coale, K.H., Dam, H.G., Lewis, M.R., Lindley, S.T., McCarthy, J.J., Roman, M.R., Stoecker, D.K., Verity, P.G., White, J.R., 1997. Iron and grazing constraints on primary production in the central equatorial Pacific: an EqPac synthesis. Limnology and Oceanography 42, 405–418.

Lenton, T.M., Watson, A.J., 2000. Redfield revisited 1. Regulation of nitrate, phosphate, and oxygen in the ocean. Global Biogeochemical Cycles 14, 225–248.

Letelier, R.M., Karl, D.M., 1996. Role of *Trichodesmium* spp. in the productivity of the subtropical North Pacific Ocean. Marine Ecology Progress Series 133, 263–273.

Letelier, R.M., Karl, D.M., 1998. *Trichodesmium* spp. physiology and nutrient fluxes in the North Pacific subtropical gyre. Aquatic Microbial Ecology 15, 265–276.

Letelier, R.M., Bidigare, R.R., Hebel, D.V., Ondrusek, M., Winn, C.D., Karl, D.M., 1993. Temporal variability of the phytoplankton community structure based on pigment analyses. Limnology and Oceanography 38, 1420–1437.

Letelier, R.M., Dore, J.E., Winn, C.D., Karl, D.M., 1996. Seasonal and interannual variations in photosynthetic carbon assimilation at station ALOHA. Deep-Sea Research II 43, 467–490.

Mague, T.H., Mague, F.C., Holm-Hansen, O., 1977. Physiology and chemical composition of nitrogen fixing phytoplankton in the central North Pacific Ocean. Marine Biology 41, 213–227.

McCarthy, J.J., Carpenter, E.J., 1979. *Oscillatoria* (*Trichodesmium*) *thiebauti* (cyanophyta) in the central North Atlantic Ocean. Journal of Phycology 15, 75–82.

Mulholland, M.R., Ohki, K., Capone, D.G., 1999. N utilization and metabolism relative to patterns of N_2 fixation in cultures of *Trichodesmium* NIBB1067. Journal of Phycology 35, 788–977.

Neumann, T., 2000. Towards a 3D-ecosystem model of the Baltic Sea. Journal of Marine Systems 25, 405–419.

OCTET Report, 2000. Proceedings of a Workshop, http://msrc.sunysb.edu/octet/.

Ohki, K., Zehr, J.P., Falkowski, P.G., Fujita, Y., 1991. Regulation of nitrogen fixation by different nitrogen sources in the marine non-heterocystous cyanobacterium *Trichodesmium* sp. NIBB1067. Archives for Microbiology 156, 335–337.

Orcutt, K., Lipschultz, F., Gunderson, K., Arimoto, R., Michaels, A.F., Knap, A.H., Gallon, J., 2001. A seasonal study of the significance of N_2 fixation by *Trichodesmium spp*. at the Bermuda Atlantic Time-series Study (BATS) site. Deep-Sea Research II 48, 1583–1608.

Oschlies, A., Garçon, V., 1999. An eddy-permitting coupled physical–biological model of the North Atlantic 1. Sensitivity to advection numerics and mixed layer physics. Global Biogeochemical Cycles 13, 135–160.

Paerl, H.W., Prufert-Bebout, L.E., Guo, C., 1994. Iron-stimulated N_2 fixation and growth in natural and cultured populations of the planktonic marine cyanobacteria *Trichodesmium* spp. Applied and Environmental Microbiology 60, 1044–1047.

Paulson, C.A., Simpson, J.J., 1977. Irradiance measurements in the upper ocean. Journal of Physical Oceanography 7, 952–956.

Payne, R.E., 1972. Albedo at the sea surface. Journal of Atmospheric Science 29, 959–970.

Price, J.F., Weller, R.A., Pinkel, R., 1986. Diurnal cycling: Observations and models of the upper ocean response to diurnal heating, cooling, and wind mixing. Journal of Geophysical Research 91, 8411–8427.

Rueter, J.G., Ohki, K., Fujita, Y., 1990. The effect of iron nutrition on photosynthesis and nitrogen fixation in cultures of *Trichodesmium* (cyanophycaea). Journal of Phycology 26, 30–35.

Rueter, J.G., Hutchins, D.A., Smith, R.W., Unsworth, N.L., 1992. Iron nutrition of *Trichodesmium*. In: Carpenter, E.J., et al. (Ed.), Marine Pelagic Cyanobacteria: *Trichodesmium* and Other Diazotrophs. Kluwer Academic Publishers, Netherlands, pp. 289–306.

Spitz, Y.H., Moisan, J.R., Abbott, M.R., 2001. Configuring an ecosystem model using data from the Bermuda-Atlantic Time Series (BATS). Deep-Sea Research II 48, 1733–1768.

Tyrrell, T., 1999. The relative influences of nitrogen and phosphorus on oceanic primary production. Nature 400, 525–531.

Wada, E., Hattori, A., 1991. Nitrogen in the Sea: Forms, Abundances and Rate Processes. CRC Press, Boca Raton, FL, pp. 208.

Wasmund, N., 1997. Occurrence of cyanobacterial blooms in the Baltic Sea in relation to environmental conditions. Internationale Revue der gesamten Hydrobiologie 82, 169–184.

Winn, C.D., Campbell, L., Christian, J., Letelier, R.M., Hebel, D.V., Dore, J.E., Fujieki, L., Karl, D.M., 1995. Seasonal variability in the phytoplankton community of the North Pacific subtropical gyre. Global Biogeochemical Cycles 9, 605–620.

Wu, J., Boyle, E., Sunda, W., Wen, L., 2001. Soluble and colloidal iron in the oligotrophic North Atlantic and North Pacific. Science 293, 847–849.

Wu, J., Sunda, W., Boyle, E.A., Karl, D.M., 2000. Phosphate depletion in the western North Atlantic Ocean. Science 289, 759–762.

Yentsch, C.M., Yentsch, C.S., Perras, J.P., 1972. Alkaline phosphatase activity in the tropical marine blue-green alga, *Oscillatoria erythraea* (*''Trichodesmium''*). Limnology and Oceanography 17, 772–774.